CHAPTER 5

EFFECT OF ULTRASONIC SHOT PEENING ON LOW CYCLE FATIGUE BEHAVIOR

5.1 Introduction

This chapter presents the effect of the duration of ultrasonic shot peening on Low cycle fatigue (LCF) life of the peak aged 7075 aluminium alloy. The results are discussed in terms of increase in the resistance of the material against fatigue crack initiation due to grain refinement in the surface region and the associated compressive stresses resulting from USSP. The USSP was performed in gage section of the cylindrical samples with hard steel balls of 3 mm diameter for different durations of 30, 60, 180 and 300 seconds at a constant amplitude of 80 μm. LCF tests were conducted under total strain control mode with triangular wave form and fully reversed axial loading (R = -1), at total strain amplitudes of ±0.38%, ±0.40%, ±0.45%, ±0.50%, ±0.55% and ±0.60%, at a constant strain rate of 5x10^{-3} s^{-1}. The un-shot peened samples are designated as un-USSP whereas those subjected to ultrasonic shot peening for 30, 60, 180 and 300 second are designated as USSP 30, USSP 60, USSP 180 and USSP 300 respectively. The microstructure in surface region of the USSP treated specimens is found to be nanostructured. The effect of surface roughness and the compressive residual stress induced by USSP is examined on LCF behavior of the alloy. Enhancement in LCF life is observed by USSP treatment up to the duration of 180 seconds, however, fatigue life was reduced from longer duration

of USSP for 300 seconds. The enhancement in LCF life is from combined effects of the surface nanostructure and the associated compressive residual stresses.

5.2 Cyclic Stress Response

The cyclic stress response of the different specimens with number of cycles, at different total strain amplitudes, is shown in Fig. 5.1. In the un-USSP condition there is tendency of mild softening from the beginning and till the end, at the higher strain amplitudes of ±0.50% to ±0.60% whereas there is cyclic hardening during the initial 100 cycles followed by stabilization and finally rapid softening at the lower strain amplitudes (Fig. 5.1a). The effect of the duration of USSP on the cyclic stress response is shown in Fig. 5.1 (b-e). It may be seen that there is cyclic hardening in all the USSP treated specimens, irrespective of the duration of USSP at all the strain amplitudes investigated. The degree of cyclic hardening is increased with increase in the total strain amplitude.

The cyclic hardening behavior exhibited by this alloy in the different conditions is also examined by the cyclic hardening factor (H_σ), the ratio of cyclic stress amplitude at any cycle to that at the first cycle $\frac{\Delta\sigma}{2}N/\frac{\Delta\sigma}{2}N_1$, with the number of cycles at the total strain amplitude of ±0.38% (Fig. 5.2). The value of H_σ increases with number of cycles and displays maximum and minimum values for the USSP 180 and the un-USSP specimens respectively. The cyclic hardening factor as well as the fatigue life increased with increase in the USSP duration except for the USSP 300.

The variation of fatigue life with USSP duration for the different total strain amplitudes is shown in Fig. 5.3. Fatigue life increases with increase in the duration of USSP

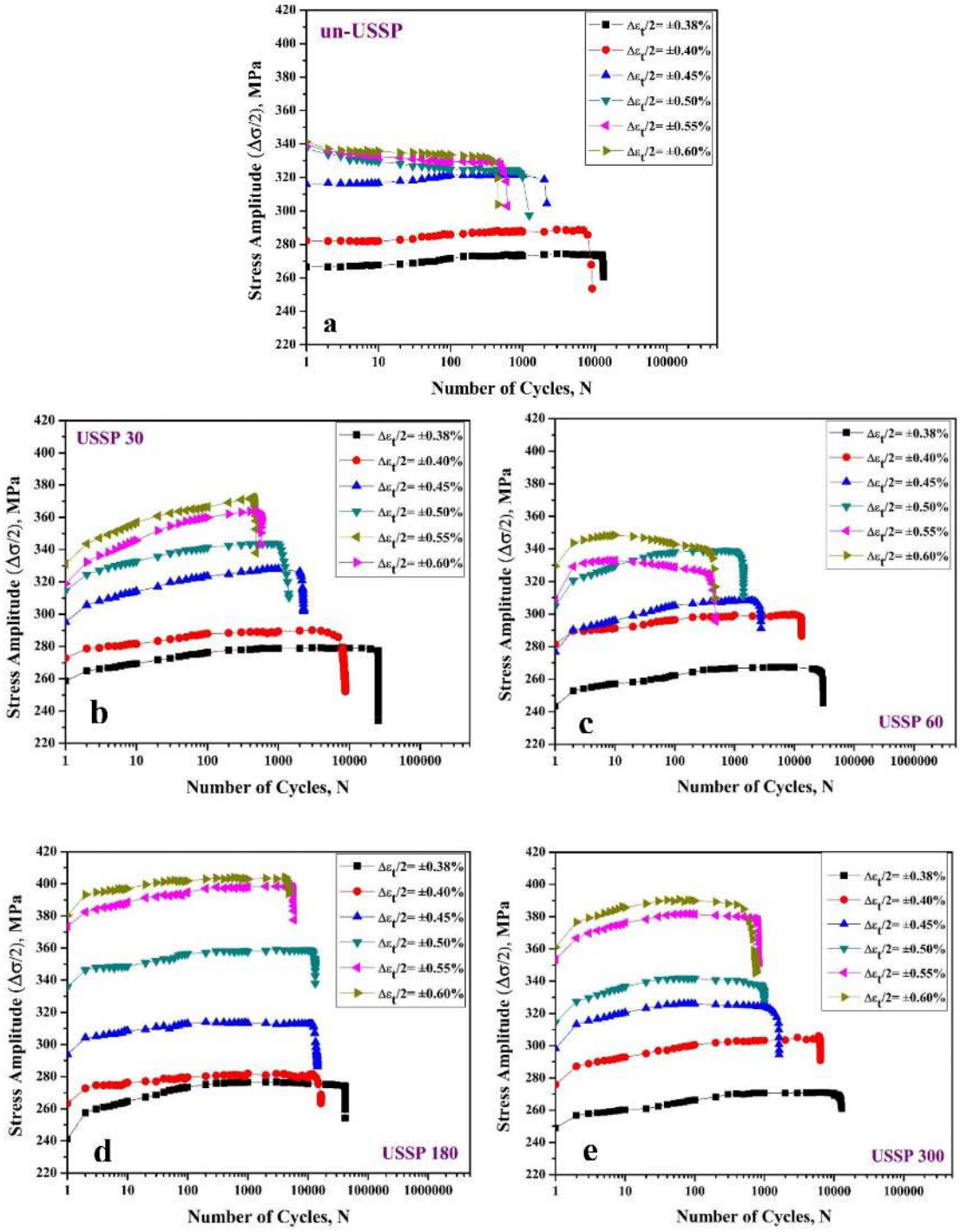

FIGURE 5.1: Cyclic Stress response curves of AA7075 in different conditions (a) un-USSP, (b) USSP 30, (c) USSP 60, (d) USSP 180 and (e) USSP 300.

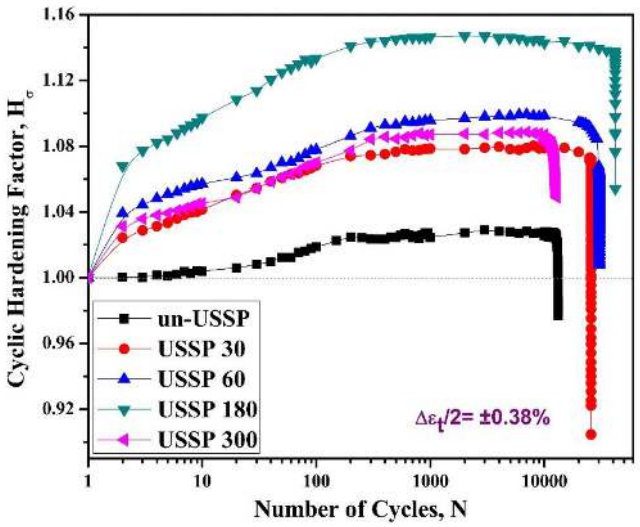

FIGURE 5.2: Variation of cyclic hardening factor with number of cycles for the un-USSP and the samples USSP treated for different durations, at the total strain amplitude $\Delta\epsilon_t/2$ of ±0.38%.

and was highest for the USSP 180 at all the strain amplitudes. The LCF life may be seen to increase progressively from USSP with lowering of the strain amplitude. There was 220% increase in fatigue life of the USSP 180 at the total strain amplitude of ±0.38% as compared with that of the un-USSP specimen.

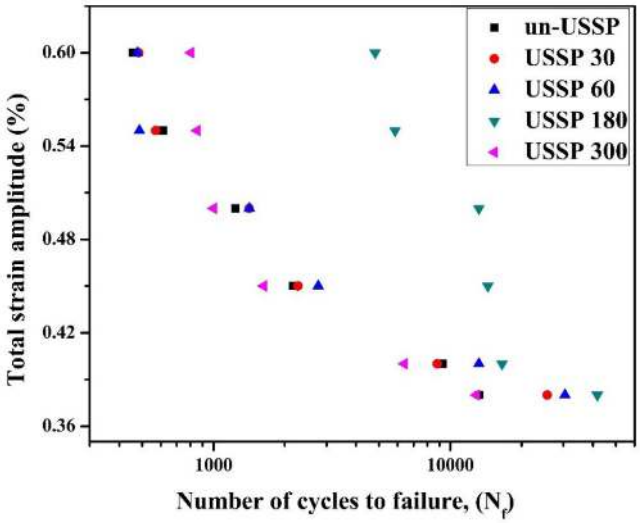

FIGURE 5.3: Dependence of fatigue life on total strain amplitude for the different conditions.

The dependence of fatigue life with plastic strain amplitude ($\Delta\epsilon_p/2$) is analyzed by the Coffin–Manson relationship [61].

$$\Delta\epsilon_p/2 = \epsilon_f^{'}(2N_f)^c \tag{5.1}$$

Where $2N_f$ is number of reversals to failure, $\epsilon_f^{'}$ and c are fatigue ductility coefficient and exponent respectively. The LCF parameters, fatigue ductility exponent and fatigue ductility coefficient are the slope and intercept on Y-axis at $2N_f$ = 1 respectively, these were determined by least square linear fit of the data in Fig. 5.4. The Coffin-Manson plots for the specimens subjected to different durations of USSP, along with that of the un-USSP specimen are shown in Fig. 5.4.

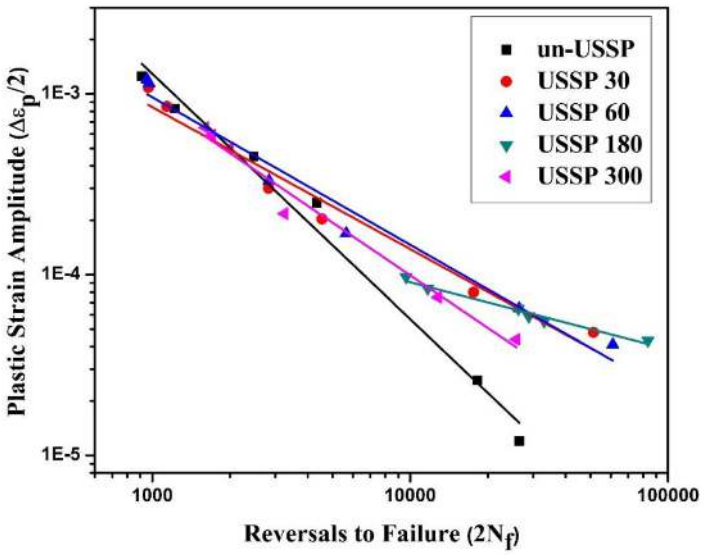

FIGURE 5.4: Dependence of fatigue life, number of reversals to failure ($2N_f$ = 1) on the plastic strain amplitude for the un-USSP and different USSP treated conditions.

The LCF parameters determined from the plots in Fig. 5.4 are presented in the Table 5.1. The high LCF resistance of the USSP 180 is reflected by the much lower value of

TABLE 5.1: LCF parameters calculated from Coffin-Manson plot for un-USSP and different USSP treated conditions.

Treatment Condition	$\epsilon_f^{'}$	**c**
un-USSP	0.065	1.35
USSP 30	0.191	0.78
USSP 60	0.270	0.81
USSP 180	0.002	0.37
USSP 300	0.130	0.74

the fatigue ductility coefficient (c).

The variation of fatigue life is also analyzed based on the plastic energy density ($\Delta W_p/2$) using the Halford-Marrow relationship [133].

$$\Delta W_p/2 = W_f^{'}(2N_f)^{\gamma} \tag{5.2}$$

where $W_f^{'}$ and γ are plastic strain energy density coefficient and exponent respectively. The plot of the plastic strain energy density versus $2N_f$ is shown in Fig. 5.5. It may

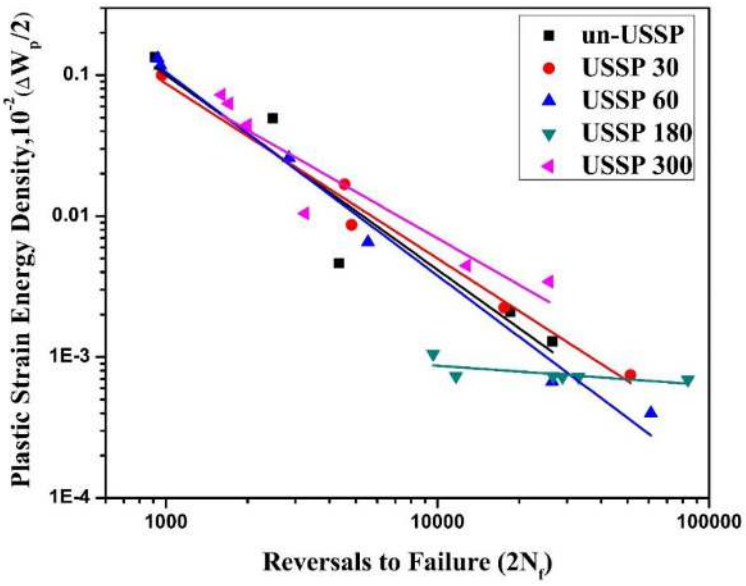

FIGURE 5.5: Variation of plastic strain energy density in un-USSP and different USSP treated conditions.

be seen that the plastic strain energy for the USSP 180 is much lower at all the strain amplitudes.

5.3 Fracture Behavior

Fracture surfaces of the un-USSP and USSP 180 specimens, tested at the different total strain amplitudes of ±0.60%, ±0.45% and ±0.38% are shown in Fig. 5.6 (a, b, c) and (d, e, f) respectively. Fatigue striations and micro-cliffs may be seen in the region of stable fatigue crack propagation. The direction of fatigue crack propagation is shown by arrows. The crack propagation path for the USSP 180 sample was more tortuous than that of the un-USSP. Secondary cracks (SC) may also be seen on fracture surface of the un-USSP specimen. The interstriation spacing was relatively less in the USSP 180 than that in the un-USSP specimen.

5.4 Discussion

The cyclic stress response shows mild hardening in the un-USSP condition initially whereas there is substantial hardening in the specimens subjected to USSP. The continuous cyclic softening in the un-USSP condition at the higher total strain amplitudes of ±0.60%, ±0.55% and ±0.50% may be attributed to disordering/shearing of the precipitates by dislocations during cyclic loading [134]. The mild hardening at lower strain amplitudes of ±0.45%, ±0.40% and ±0.38% may be due to mutual interaction of dislocations as well as with the precipitates. After some cycles the dislocation structure gets stabilized and the cyclic

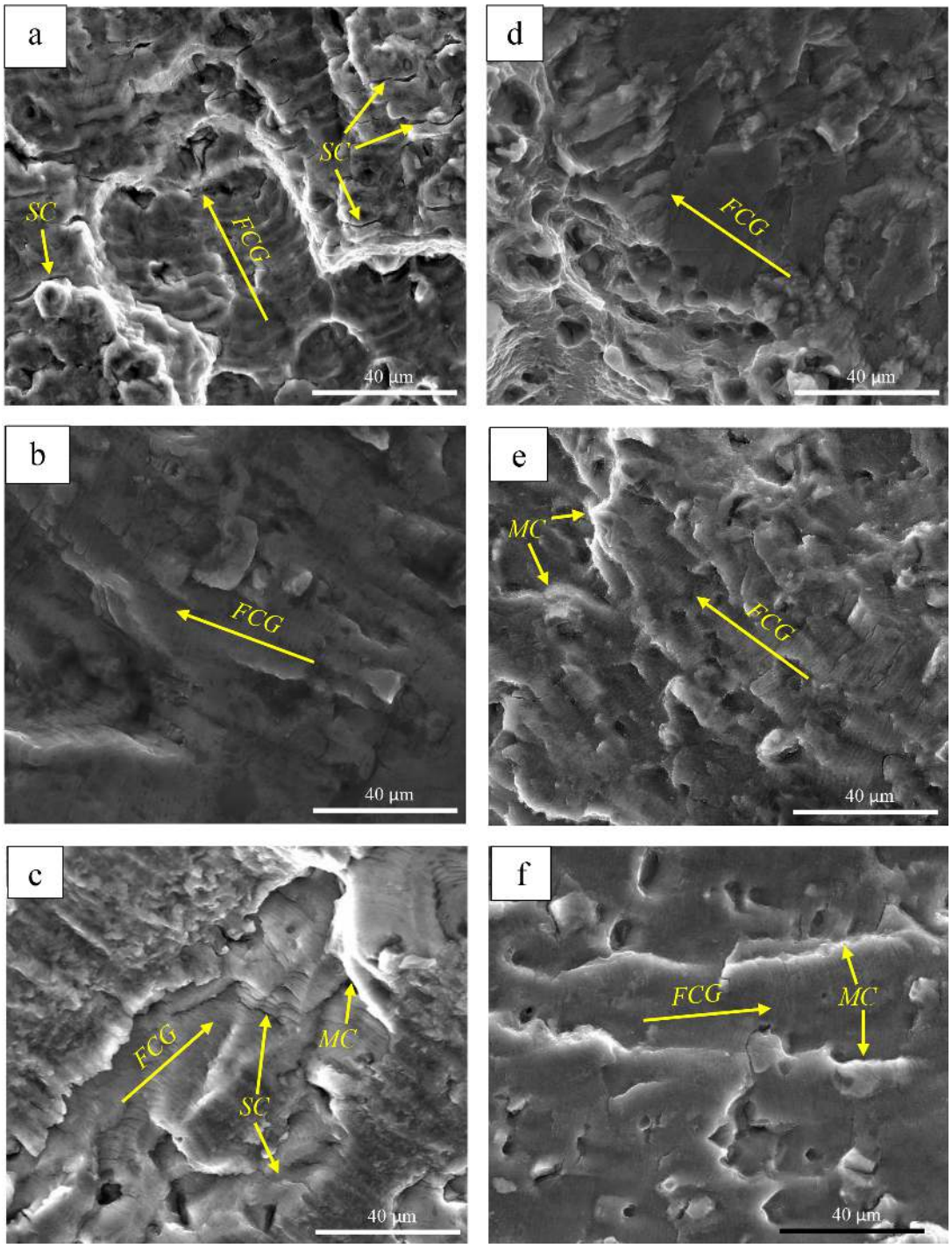

FIGURE 5.6: SEM fractographs showing morphology of fractured surfaces of the un-USSP sample, tested at the total strain amplitudes of (a) ±0.60%, (b) ±0.45%, (c) ±0.38% and the USSP 180 samples tested at the total strain amplitude of (d) ±0.60%, (e) ±0.45%, (f) ±0.38%.

stress response becomes stable [135]. On the other hand, there is cyclic hardening in the USSP treated specimens even at the higher strain amplitudes, in contrast to softening in the un-USSP specimens, irrespective of the duration of USSP. It may be attributed to the effects of grain refinement and work hardening in surface region of the USSP treated specimens. The degree of hardening increased with the duration of USSP and it was maximum for the USSP 180 specimens. The relatively lower degree of cyclic hardening in the USSP 300 specimens than those in the USSP 180 may be attributed to the higher roughness and damage of the surface in the former condition.

The substantial enhancement in LCF life of the USSP 180 specimens over the entire range of strain amplitudes studied is due to combined effect of the nanostructured surface layer, the associated compressive residual stresses and damage of the surface. The values of residual stresses of the USSP 180 specimens, in the as-USSP treated (un-tested) condition, and of those following LCF tests at different total strain amplitudes, upto their respective half-lives, are shown in Fig. 5.7.

It may be seen that prior to LCF testing the magnitude of the compressive residual stress was -226 MPa and it was reduced to -161 MPa, -198 MPa and -206 MPa due to LCF testing to their half-lives at $\Delta\epsilon_p/2$= ±0.6%, ±0.5% and ±0.38%, respectively. It is obvious that the magnitude of the compressive residual stress is marginally lowered at the lower strain amplitudes of ±0.38% and ±0.50% and the decrease is relatively more at the highest strain amplitude of ±0.60%.

It may thus be seen that there was very less relaxation in the compressive residual stresses even after the half LCF lives at the different total strain amplitudes. Mikova et. al

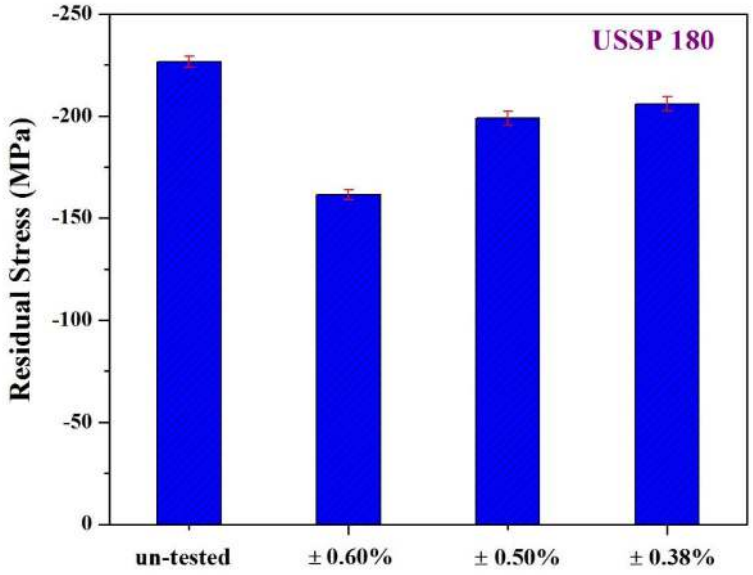

FIGURE 5.7: Compressive residual stress in surface region of the USSP 180 specimen in the as-USSP treated condition and following LCF at different total strain amplitudes up to half of their LCF life ($N_f/2$).

[136] observed that magnitude of the residual stress of the severely shot peened (SSP) X70 microalloyed steel was almost same in the surface region even after its LCF testing but the depth of the region associated with the compressive stress was reduced in comparison with that of the un-tested condition. Also, the surface roughness of the specimen plays an important role on fatigue life because fatigue cracks are known to initiate from surface of the specimen. Though there was increase in surface roughness due to USSP the resulting nanostructured surface layer associated with high compressive residual stress overcame the deleterious effect of the surface roughness [136]. Fig. 5.7 shows marked difference in interstriation spacings on fractured surfaces of the un-USSP and USSP treated specimens, tested at identical strain amplitudes. The more closely spaced striations and tortuousness in crack propagation path for the USSP treated specimens reflect high resistance against fatigue crack propagation (Fig. 5.7). It is interesting to note from the fractographs in

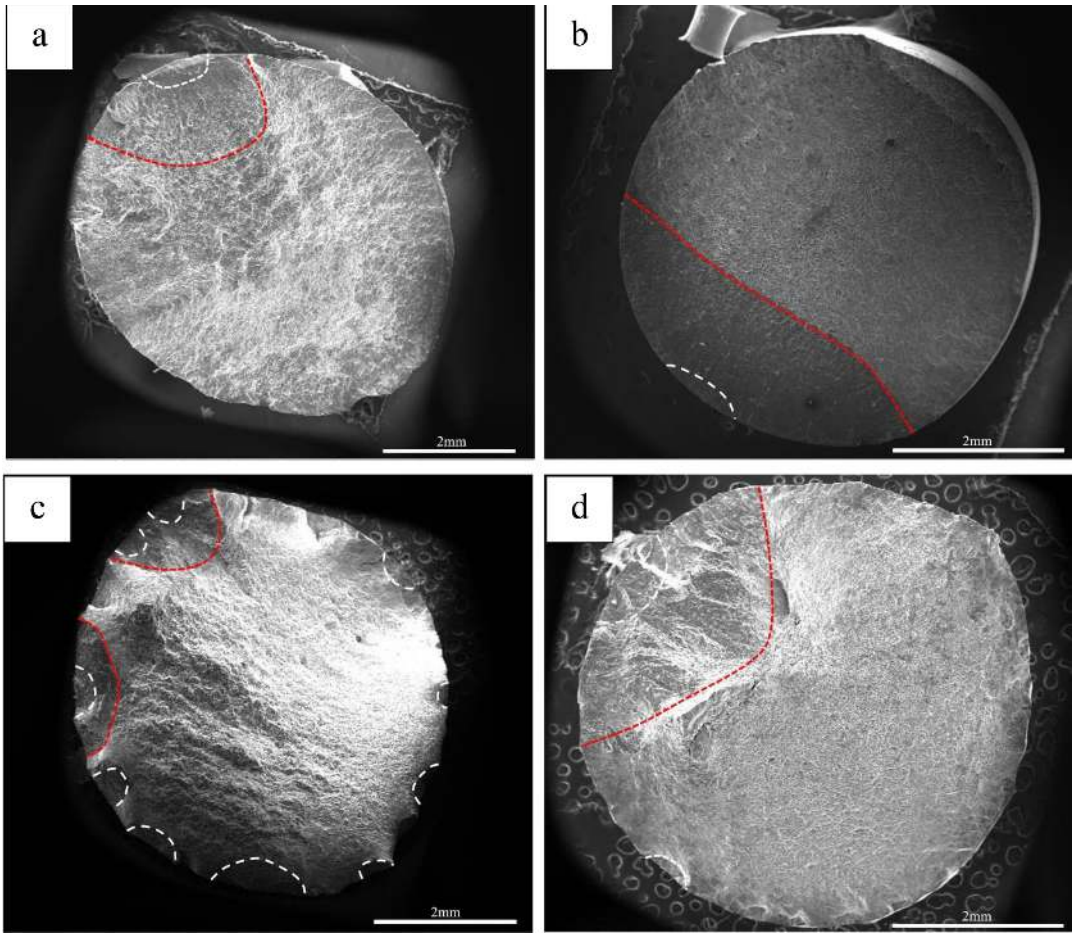

FIGURE 5.8: SEM fractographs showing fracture surfaces of the specimens tested at the total strain amplitudes of ±0.38%, ±0.60% respectively: (a, b) un-USSP and (c, d) USSP 180.

Fig. 5.8 that the number density of crack initiation sites (marked in white) is higher in the USSP 180 specimen as compared with that of the un-USSP, it implies that the average stress intensity factor at the crack tips in the USSP 180 specimen would have been less than that in the un-USSP condition and thus the higher fatigue life of the USSP 180 may be understood. Fatigue cracks are known to initiate from slip bands at the surface hence it is likely that the process of fatigue crack initiation from surface of the USSP treated specimen would have been delayed due to surface nanostructuring.

Further, the gradient microstructure associated with high compressive residual stress

in the sub-surface has been reported to retard the rate of fatigue crack propagation [137, 138]. Also, in the samples with gradient nano structure (GNS) large ductility can be attained by suppressing strain localization [139]. Deformation is relatively more homogeneous in the USSP treated surface layer and is heterogeneous in the un-USSP specimen because of the formation of large slip bands in the coarse surface grains, favorably oriented to stress axis. Also the process of crack initiation from the surface is delayed in the USSP 180 condition due to the relatively more homogeneous deformation.

The relatively less pronounced effect of shorter durations of USSP in the USSP 30 and USSP 60 specimens in comparison with that of the USSP 180, on their fatigue lives may be attributed to comparatively less thickness of the nanostructured surface region and the lower compressive stresses associated with them. During the lower duration of USSP treatment, initially there is formation of dimple like features which increase the roughness of the surface. However, with increase in the duration of USSP the entire surface gets covered with overlapping dimples, however, with further increase in the duration of USSP the roughness does not increase, rather gets stabilized [98]. In the case of higher surface roughness, the surface layer with ultrafine grains and deeper compressive residual stress is able to overcome the adverse effect of increased roughness [140]. Bagherifard et. al [141] observed that severe shot peening (SSP) with balls of 0.70 mm diameter caused deterioration in fatigue life of cast iron due to high surface roughness. However, repeening of the specimens with balls of small diameter of 0.28 mm enhanced the fatigue life by 67% with respect to that of the un-peened specimen, inspite of the high roughness. It was attributed to presence of thicker nanocrystallized surface layer, high compressive residual

stress and the work hardened surface.

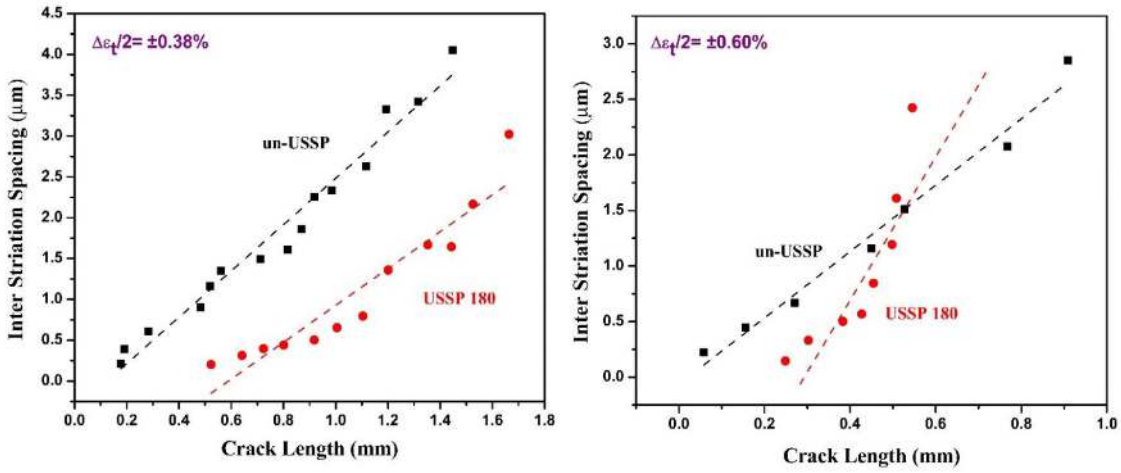

FIGURE 5.9: Variation of interstriation spacing at different total strain amplitudes for the un-USSP and USSP 180 specimens.

The effect of USSP on fatigue crack growth behavior of the un-USSP and USSP 180 specimen may be visualized from the plots in Fig. 5.9, showing variation of interstriation spacings with crack length for the respective conditions. It can be concluded from these plots that USSP treatment was more effective at lower strain amplitudes, near the HCF regime.

The relatively lower fatigue life of the USSP 300 specimens compared with that of the USSP 180 may be attributed essentially to higher roughness in the former condition and the consequent localization of the stress. It may be seen from the micrograph in Fig. 5.10(a) that surface of the USSP 300 specimen is highly uneven and also there are several cracks, as shown by arrows.

Such features on the surface cause high stress concentration and enhance the process of fatigue crack initiation as well as the rate of crack propagation. The deleterious effect

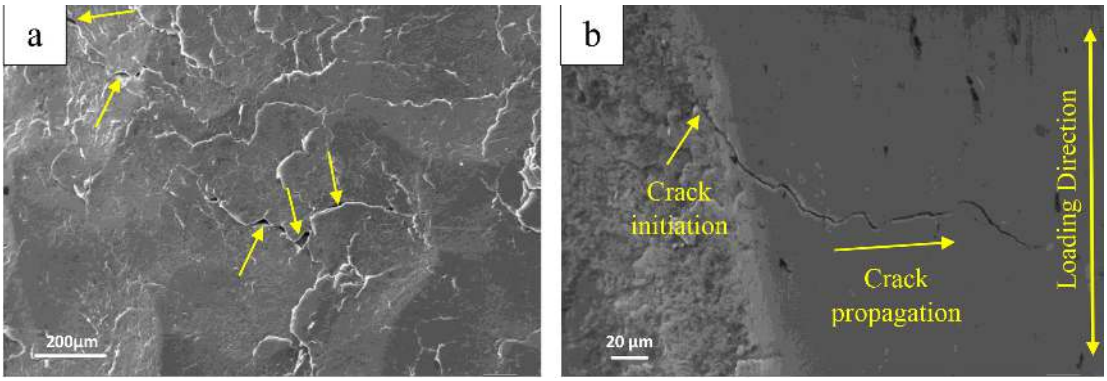

FIGURE 5.10: SEM micrograph of the USSP 300 sample tested in LCF at the total strain amplitude of ±0.38%. (a) Surface morphology of the circumferential surface close to fracture end and (b) longitudinal section of the tested sample showing crack profile.

of high surface roughness on LCF is quite evident from Fig. 5.10(b) showing crack initiation at the site of stress concentration (yellow arrow) on the rough surface of the USSP 300 specimen and its growth inside the specimen, normal to the stress axis on machined flat surface of the specimen tested in LCF. It is relevant to mention that residual compressive stress was higher in the USSP 300 than that in the USSP 180, however, LCF life of the USSP 300 specimens was less than that of the USSP 180 in spite of its residual compressive stress being higher. Obviously, it was due to more detrimental effect of the surface roughness than the beneficial effect of the residual compressive stress. The findings of lower fatigue life in the present investigation from longer duration of USSP are in line with the earlier observations made on austenitic stainless steel [62]. The roughness/cracking at the surface resulting from long duration of USSP for 300 seconds would have reduced also the associated compressive stresses in those regions because of relaxation hence the effectiveness of the compressive residual stress in enhancing fatigue life was reduced. Thus, it is seen that enhancement of fatigue life from USSP is maximum for the optimum condition of USSP.

5.5 Conclusions

The following conclusions are drawn from this chapter:

1. Initially there was mild cyclic softening at high strain amplitudes, followed by stabilization of the cyclic stress in the un-USSP condition whereas, there was initially cyclic hardening in the USSP treated condition followed by stabilised stress response at all the strain amplitudes studied.

2. Pronounced enhancement in LCF life resulted from the USSP treatment for 180 seconds.

3. Enhancement in LCF life in the USSP 180 was due to combined beneficial effect of grain refinement in the surface region and the associated compressive residual stresses without damage of the treated surface.

4. USSP treatment for 300 seconds (USSP 300) caused damage to the surface, cracks were developed and fatigue life was reduced.